The cross-correlation of the CMB polarization and the 21-cm line fluctuations from cosmic reionization

Hiroyuki Tashiro, Nabila Aghanim, Mathieu Langer, Marian Douspis, Saleem Zaroubi

Mon. Not. R. Astron. Soc. **489,** 469–477 (2008) doi:10.1111/j.1365-2966.2008.13606.x

The cross-correlation of the CMB polarization and the 21-cm line fluctuations from cosmic reionization

Hiroyuki Tashiro,[1,2]★ Nabila Aghanim,[1,2] Mathieu Langer,[1,2] Marian Douspis[1,2] and Saleem Zaroubi[3]

[1] *Institut d'Astrophysique Spatiale (IAS), Bâtiment 121, F-91405, Orsay, France*
[2] *Université Paris-Sud XI and CNRS (UMR 8617), France*
[3] *Kapteyn Astronomical Institute, Landleven 12, Groningen 9747 AD, the Netherlands*

Accepted 2008 June 17. Received 2008 June 9; in original form 2008 February 26

ABSTRACT

The cosmic microwave background (CMB) polarization and the 21-cm line fluctuations are powerful probes of cosmological reionization. We study how the cross-correlation between the CMB polarization (*E* modes) and the 21-cm line fluctuations can be used to gain further understanding of the reionization history, within the framework of inhomogeneous reionization. Since the *E*-mode polarization reflects the amplitude of the quadrupole component of the CMB temperature fluctuations, the angular power spectrum of the cross-correlation exhibits oscillations at all multipoles. The first peak of the power spectrum appears at the scale corresponding to the quadrupole at the redshift, which is probed by the 21-cm line fluctuations. The peak reaches its maximum value in redshift when the average ionization fraction of the universe is about half. On the other hand, on small scales, there is a damping that depends on the duration of reionization. Thus, the cross-correlation between the CMB polarization and the 21-cm line fluctuations has the potential to accurately constrain the epoch and the duration of reionization.

Key words: cosmology: theory – large-scale structure of Universe.

1 INTRODUCTION

The history of the cosmological reionization is one of the open problems of modern cosmology. Questions like what causes the reionization and how it proceeds are intimately related to the evolution of matter density fluctuations and to the formation of the first structures (Barkana & Loeb 2001). The lack of observational data makes it quite difficult to answer these questions today. Up to now, the available probes of the reionization epoch are just a few, for example, the Gunn–Peterson test (Gunn & Peterson 1965) and the cosmic microwave background (CMB) radiation, in particular its polarization (Zaldarriaga 1997). The observation of the Gunn–Peterson effect, which probes the amount of neutral hydrogen, suggests that full reionization was accomplished by $z \sim 6$ (Fan et al. 2006). The CMB polarization, in turn, measures the optical depth of the Thomson scattering from the last scattering surface to the present epoch. The *Wilkinson Microwave Anisotropy Probe* (*WMAP*) 3 yr data provide an optical depth $\tau \sim 0.09$ (Page et al. 2007) suggesting that the reionization began around $z = 10$.

In addition to those two probes, the observation of fluctuations of the 21-cm line background is expected to be one of the most promising methods to study reionization (Madau, Meiksin & Rees 1997; Tozzi et al. 2000; Ciardi & Madau 2003). The 21-cm line corresponds to the energy of the hyperfine spin flip transition of neutral hydrogen atoms. After decoupling of the baryon temperature from the CMB temperature around $z \sim 300$, neutral hydrogen atoms absorb or emit a 21-cm line, depending on their temperature. Since the 21-cm line is redshifted by the cosmological expansion, we can obtain redshift slices of the Universe by choosing the frequency of the observation. It is thus possible to follow the evolution of the intergalactic medium before and during reionization directly. The 21-cm line observations have recently gained a lot of attention (Loeb & Zaldarriaga 2004; Furlanetto, Oh & Pierpaoli 2006; Tashiro & Sugiyama 2006; Cooray 2006), and several projects are designed for measuring the fluctuating line background [e.g. Murchison Widefield Array (MWA),[1] LOw Frequency ARray (LOFAR)[2] and Square Kilometre Array (SKA)[3]].

★E-mail: hiroyuki.tashiro@ias.u-psud.fr
[1] http://web.haystack.mit.edu/array/MWA
[2] http://www.lofar.org
[3] http://www.skatelescope.org

In the near future, we will therefore have different direct and complementary probes of reionization. We thus expect that cross-correlations between them will provide even more information than their respective autocorrelations. This is the case especially for the cross-correlation between the CMB temperature anisotropies and the 21-cm line fluctuations on large scales ($\ell \sim 100$ – Alvarez et al. 2006; Adshead & Furlanetto 2008) and on small scales ($\ell > 1000$ – Cooray 2004; Salvaterra et al. 2005; Slosar, Cooray & Silk 2007). Since the observations of the 21-cm lines are expected to be dominated by foregrounds and noise (Jelic et al. 2008), calculating the cross-correlation is indeed a good way to extract information on reionization. In particular on large scales, the 21-cm line fluctuations are correlated with the CMB Doppler temperature anisotropies, which are due to the motion of ionized baryons. Alvarez et al. (2006) showed that the maximum amplitude of the cross-correlation is reached at the redshift when the ionized fraction is one-half, which potentially provides a way to constrain double reionization models (e.g. Cen 2003).

In this study, we examine the cross-correlation between the CMB *E*-mode polarization (a more effective probe than the temperature anisotropies) and the fluctuations of the 21-cm line background on large scales. Measuring *E*-mode polarization is one of the present challenging observations for CMB experiments. However, projects like PLANCK and CMB-pol will provide precise CMB polarization maps in the near future. Similarly, cosmological observation of 21-cm line background is still belongs to the future, but LOFAR and MWA are being completed and will soon provide us with maps of neutral hydrogen at high redshifts. Hence, it is useful to investigate what information on reionization we can extract from the cross-correlation of those maps. Indeed, we show here that the cross-correlations are a potentially powerful tool to constrain the history of cosmic reionization. This article is organized as follows. In Section 2, we provide the analytic formula of the cross-correlation between the CMB *E*-mode polarization and the fluctuations of the 21-cm line background. In Section 3, we show and discuss the results of the cross-correlation. Section 4 is devoted to the conclusions. Throughout the paper, we use *WMAP* 3-yr values for the cosmological parameters, i.e. $h = 0.73$ ($H_0 = h \times 100\,\mathrm{km\,s^{-1}\,Mpc^{-1}}$), $T_0 = 2.725$ K, $h^2\,\Omega_\mathrm{b} = 0.0223$ and $h^2\,\Omega_\mathrm{m} = 0.128$ (Spergel et al. 2007) for a flat cosmology. We also set the speed of light to $c = 1$.

2 CROSS-CORRELATION BETWEEN CMB *E*-MODE POLARIZATION AND 21-CM LINES

2.1 The CMB *E*-mode polarization

The CMB polarization is best described by the Stokes parameters, Q and U. Since the Stokes parameters have spin-2, they can be decomposed on to the plane waves and spin-2 spherical harmonics ${}_{\pm2}Y^m_\ell$ (Hu & White 1997),

$$(Q \pm iU)(\eta, \boldsymbol{x}, \hat{\boldsymbol{n}}) = \sum_{\ell\, m} (-i)^\ell \sqrt{\frac{4\pi}{2\ell+1}} \int \frac{d^3k}{(2\pi)^3} \left(E^{(m)}_\ell \pm i\, B^{(m)}_\ell\right) \exp(i\boldsymbol{k}\cdot\boldsymbol{x})\, {}_{\pm2}Y^m_\ell(\hat{\boldsymbol{n}}). \tag{1}$$

Here, $m = 0, \pm1$ and ±2 correspond to the scalar, vector and tensor types. In this paper, we only consider $m = 0$ modes because they dominate other polarization modes at the scales we are interested in.

The CMB polarization components, $E^{(0)}_\ell$ and $B^{(0)}_\ell$, are obtained from the Boltzmann equations for CMB. According to those, $B^{(0)}_\ell = 0$ for all ℓs and the evolution of $E^{(0)}_\ell$ is given by the following integral solution,

$$\frac{E^{(0)}_\ell(\eta_0, k)}{2\ell+1} = -\frac{3}{2}\sqrt{\frac{(\ell+2)!}{(\ell-2)!}} \int_0^{\eta_0} \mathrm{d}\eta\, \dot{\tau} e^{-\tau} P^{(0)} \frac{j_\ell(k(\eta_0-\eta))}{[k(\eta_0-\eta)]^2}, \tag{2}$$

where $P^{(0)}$ is the $m = 0$ source term due to Thomson scattering, $\dot{\tau}$ is the differential optical depth for Thomson scattering in conformal time, given by $\dot{\tau} = n_\mathrm{e}\sigma_\mathrm{T}a$ with the electron number density n_e, the cross-section of Thomson scattering σ_T and the scale factor a normalized to the present epoch, and τ is the optical depth between the conformal times η and η_0. The source term $P^{(0)}$ is related to the initial gravitational potential Φ_0 via the transfer function $D_E(k, \eta)$,

$$P^{(0)} = D_E(k, \eta)\Phi_0. \tag{3}$$

We provide the detailed calculation of the transfer function in the appendix.

We also define the E modes in the direction $\hat{\boldsymbol{n}}$ on the sky by

$$E(\hat{\boldsymbol{n}}) = \sum_{\ell\, m} (-i)^\ell \sqrt{\frac{4\pi}{2\ell+1}} \int \frac{d^3k}{(2\pi)^3} E^{(0)}_\ell Y^m_\ell(\hat{\boldsymbol{n}}). \tag{4}$$

2.2 21-cm line fluctuations

The observed brightness temperature of the 21-cm lines in a direction $\hat{\boldsymbol{n}}$ and at a frequency ν is given as in Madau et al. (1997) by

$$T_{21}(\hat{\boldsymbol{n}}; \nu) = \frac{\tau_{21}}{(1+z_\mathrm{obs})}(T_\mathrm{s} - T_\mathrm{CMB})[\eta_\mathrm{obs}, \hat{\boldsymbol{n}}(\eta_0 - \eta_\mathrm{obs})]. \tag{5}$$

Here, the conformal time η_obs refers to the redshift z_obs that satisfies $\nu = \nu_{21}/(1+z_\mathrm{obs})$ with ν_{21} being the frequency corresponding to the 21-cm wavelength. The optical depth for the 21-cm line absorption is

$$\tau_{21} \sim 8.6 \times 10^{-3} x_\mathrm{H} \frac{T_\mathrm{cmb}}{T_\mathrm{s}} \left(\frac{\Omega_\mathrm{b}h^2}{0.02}\right) \left[\left(\frac{0.15}{\Omega_\mathrm{m}h^2}\right)\left(\frac{1+z_\mathrm{obs}}{10}\right)\right]^{1/2}, \tag{6}$$

where $x_{\rm H}$ is the fraction of neutral hydrogen, and $T_{\rm s}$ is the spin temperature given by the ratio of the number density of hydrogen atoms in the excited state to that of hydrogens in the ground state.

Equations (5) and (6) show that the observed brightness temperature of the 21-cm lines will reflect the baryon density fluctuations $\delta_{\rm b}$ and the fluctuations of the ionized fraction $\delta_{\rm x}$. We can rewrite equation (5) in the linear approximation for both $\delta_{\rm b}$ and δ_x as

$$T_{21}(\hat{\boldsymbol{n}};\nu) = [1-\bar{x}_{\rm e}(1+\delta_x)](1+\delta_{\rm b})T_0, \tag{7}$$

where $x_{\rm e} = 1 - x_{\rm H}$ is the ionized fraction and

$$T_0 = 23\left(\frac{\Omega_{\rm b}h^2}{0.02}\right)\left[\left(\frac{0.15}{\Omega_{\rm m}h^2}\right)\left(\frac{1+z_{\rm obs}}{10}\right)\right]^{1/2}\ {\rm mK}. \tag{8}$$

Here, we assume that $T_{\rm s}$ is much larger than the CMB temperature which is valid soon after the beginning of the reionization (Ciardi & Madau 2003).

After performing the Fourier transform of equation (7), we obtain the 21-cm line fluctuations,

$$\begin{aligned}\delta T_{21}(\hat{\boldsymbol{n}};\nu) &\equiv T_{21}(\hat{\boldsymbol{n}};\nu) - T_0 \\ &= T_0\int\frac{{\rm d}k^3}{(2\pi)^3}\left[(1-\bar{x}_{\rm e})\delta_{\rm b} - \bar{x}_{\rm e}\delta_x\right]\exp\left\{-i\boldsymbol{k}\cdot[(\eta-\eta_{\rm obs})\hat{\boldsymbol{n}}]\right\}.\end{aligned} \tag{9}$$

Therefore, the 21-cm line fluctuation map at the frequency ν can be described by

$$\delta T_{21}(\hat{\boldsymbol{n}};\nu) = T_0\sum_\ell\int\frac{{\rm d}k^3}{(2\pi)^3}\sqrt{4\pi(2\ell+1)}\left[(1-\bar{x}_{\rm e})(1+F\mu^2)\delta_{\rm b} - \bar{x}_{\rm e}\delta_x\right]j_\ell[k(\eta_0-\eta_{\rm obs})]Y_\ell^0(\hat{\boldsymbol{n}}), \tag{10}$$

where we applied Rayleigh's formula to equation (9),

$$\exp(-i\boldsymbol{k}\cdot\boldsymbol{x}) = \sum_\ell\sqrt{4\pi(2\ell+1)}(-i)^\ell j_\ell(kr)Y_\ell^0(\hat{\boldsymbol{n}}), \tag{11}$$

where $\hat{\boldsymbol{n}}$ is measured in the coordinate system where $\boldsymbol{k}$ is $\hat{\boldsymbol{e}}_3$. In equation (10), we included the factor $(1+F\,\mu^2)$ to account for the enhancement of the fluctuation amplitude due to the redshift distortion (Kaiser 1987) on the 21-cm line fluctuations where $\mu = \hat{\boldsymbol{k}}\cdot\hat{\boldsymbol{n}}$ and $F = d\ln g/d\ln a$ with $g(a)$ is the linear growth factor of baryon fluctuations (Bharadwaj & Ali 2004).

2.3 Cross-correlation between 21-cm and *E*-mode fluctuations

The angular power spectrum is defined as the average of the spherical harmonic coefficients $a_{\ell m}$ over the $(2\ell+1)$ m-values,

$$C_\ell = \sum_m\frac{\langle|a_{\ell m}|^2\rangle}{(2\ell+1)}, \tag{12}$$

where the $a_{\ell m}$ is defined for an arbitrary sky map $f(\hat{\boldsymbol{n}})$ as

$$f(\hat{\boldsymbol{n}}) = \sum_{\ell m}a_{\ell m}Y_\ell^m. \tag{13}$$

From equations (4) and (10), we can thus derive the angular power spectrum of the cross-correlation between E modes and 21-cm line fluctuations:

$$\begin{aligned}C_\ell^{E-21} &= 4\pi T_0\int{\rm d}\eta\int\frac{{\rm d}k^3}{(2\pi)^3}\frac{\left\langle E_\ell^0(\eta,k)\left[(1-\bar{x}_{\rm e})(1+F\mu^2)\delta_{\rm b} - \bar{x}_{\rm e}\delta_x\right]\right\rangle}{(2\ell+1)}j_\ell(k(\eta_0-\eta_v)) \\ &= -\frac{3}{\pi}T_0\sqrt{\frac{(\ell+2)!}{(\ell-2)!}}\int{\rm d}k\int{\rm d}\eta k^2\dot{\tau}e^{-\tau}D_E(k,\eta)\left[\frac{4}{3}(1-\bar{x}_{\rm e})P_{\Phi\delta_{\rm b}} - \bar{x}_{\rm e}P_{\Phi\delta_x}\right]\frac{j_\ell[k(\eta_0-\eta_{\rm obs})]j_\ell[k(\eta_0-\eta)]}{[k(\eta_0-\eta)]^2},\end{aligned} \tag{14}$$

where $P_{\Phi\delta_{\rm b}}$ and $P_{\Phi\delta_x}$ are the power spectra of the cross-correlation between the gravitational potential and the baryon density fluctuations, and between the gravitational potential and the fluctuations of the ionized fraction, respectively. In the second line, we use $F\langle\mu^2\rangle = 1/3$ for the matter-dominated epoch.

The cosmological linear perturbation theory provides the relation between the baryon density fluctuations and the initial gravitational potential (e.g. Kodama & Sasaki 1984), $\delta_{\rm b}(k,\eta) = k^2D_{\rm b}(k,\eta)\,\Phi_0(k)$ where $D_{\rm b}$ is the transfer function of baryons. The power spectrum $P_{\Phi\delta_{\rm b}}$ can thus be written in terms of the initial power spectrum of the gravitational potential P_Φ as

$$P_{\Phi\delta_{\rm b}} = k^2D_{\rm b}(k,\eta)P_\Phi. \tag{15}$$

Although the reionization process is not well known, we can reasonably expect that there is a relation between the fluctuations of the ionized fraction and that of the matter density. Ionizing sources are formed in dense regions. They ionize the surrounding medium with an efficiency that depends on the density of the medium. This translates into two possible cases: one where ionized fluctuations and matter overdensities coincides, and one where ionized fluctuations and matter density is antibiased (e.g. Benson et al. 2001). Following Alvarez et al. (2006), we assume that the fluctuations of the ionized rate are associated with the matter density contrast using the Press–Schechter description (Press & Schechter 1974). As a result, the power spectrum $P_{\Phi\delta_x}$ is given by

$$\bar{x}_{\rm e}P_{\Phi\delta_x} = -\bar{x}_{\rm H}\ln\bar{x}_{\rm H}(\bar{b}_{\rm h}-1-f)D_{\rm m}(k,\eta)k^2P_\Phi, \tag{16}$$

where $D_{\rm m}$ is the transfer function of matter (both dark and baryonic), $\bar{b}_{\rm h}$ is the average bias of dark matter haloes more massive than $M_{\rm min}$, the minimum mass of the source of ionizing photons:

$$\bar{b}_{\rm h} = 1 + \sqrt{\frac{2}{\pi}} \frac{e^{-\delta_c^2/2\sigma^2(M_{\rm min})}}{f_{\rm coll}\sigma(M_{\rm min})}, \tag{17}$$

where $\sigma(M)$ is the variance of the density fluctuations smoothed with a top-hat filter of the scale corresponding to a mass M, and $f_{\rm coll}$ is the fraction of matter collapsed into haloes with $M > M_{\rm min}$. In this paper, we choose $M_{\rm min}$ such that the halo virial temperature is $T_{\rm vir}(M_{\rm min}) = 10^4$ K. This choice corresponds to the assumption that the ionizing sources form in dark matter haloes where the gas cools efficiently via atomic cooling. The parameter f describes the reionization regime we are interested in. For $f = 0$, we are in the 'photon-counting limit' case where recombinations are not important and where the progress of the reionization depends on the number of ionizing photons only. The overdense regions contain more collapsed objects which are sources of ionizing photons. Therefore, in this case, ionization in overdense regions is easier than in underdense regions. On the contrary, $f = 1$ indicates the 'Strömgren limit' case where ionization is balanced by recombination. Although the overdense regions contain more sources of ionizing photons, the recombination rate in overdense regions is higher than in underdense regions. Hence, overdense regions in the $f = 1$ case have a lower ionized fraction than in the $f = 0$ case (for details, see Alvarez et al. 2006).

Finally, in order to calculate equation (14), we need the evolution of the mean neutral hydrogen fraction for which we use a simple parametrization based on two key quantities, the reionization epoch (defined as the redshift at which the ionized fraction equals 0.5), $z_{\rm re}$ and the duration of reionization, Δz,

$$\bar{x}_{\rm H}(z) = \frac{1}{1 + \exp[-(z - z_{\rm re})/\Delta z]}. \tag{18}$$

In the following, we will vary both $z_{\rm re}$ and Δz, and investigate their effect on the cross-correlation signal.

3 RESULTS AND DISCUSSIONS

As one can see in equation (14), the angular power spectrum C_ℓ^{E-21} of the cross-correlation is a function of several key parameters that encode the prominent details of the reionization history. Consequently, and as we show here, the global shape of the C_ℓ^{E-21} as well as the amplitude and redshift dependence of its first peak are features that can be traced back to the reionization characteristics.

First, it is worth noting that because of the double integration of the spherical Bessel functions in equation (14), the angular power spectrum reflects the source term $P(k_{\rm obs})$, namely the quadrupole term of the CMB temperature anisotropy, at $z_{\rm obs}$ where $k_{\rm obs}$ satisfies $k_{\rm obs} = \ell/(\eta_0 - \eta_{\rm obs})$. Accordingly, the angular power spectrum of the cross-correlation exhibits its first peak at a multipole $\ell < 10$ which corresponds to the angular separation of the quadrupole at $z_{\rm obs}$. The oscillations at higher ℓs (>10) are due to the free streaming of the quadrupole at redshifts higher than $z_{\rm obs}$.

We first investigate the effect of the duration of reionization Δz. We present in the left-hand panel of Fig. 1 three cases: one corresponding to a instantaneous reionization $\Delta z = 0.01$ and two with longer durations ($\Delta z = 1$ and 2). We compute the angular spectra of the cross-correlation between 21-cm line fluctuations and the CMB E-mode fluctuations for those different durations but for the same given epoch of reionization, $z_{\rm re} = 10$, an observing redshift, $z_{\rm obs} = 10$, and in the case of the 'photon-counting limit' ($f = 0$). The difference in the duration of reionization induces both a minor and a major effects on the spectra. The minor effect is the observed shift of the peak position to higher ℓs with increasing durations. Since a longer duration increases the contribution of the visibility function $\dot{\tau}e^{-\tau}$ in equation (14), which we plot in the right-hand panel of Fig. 1, the contributions from redshifts larger than $z_{\rm obs}$ accumulate in the calculation of the integration. However,

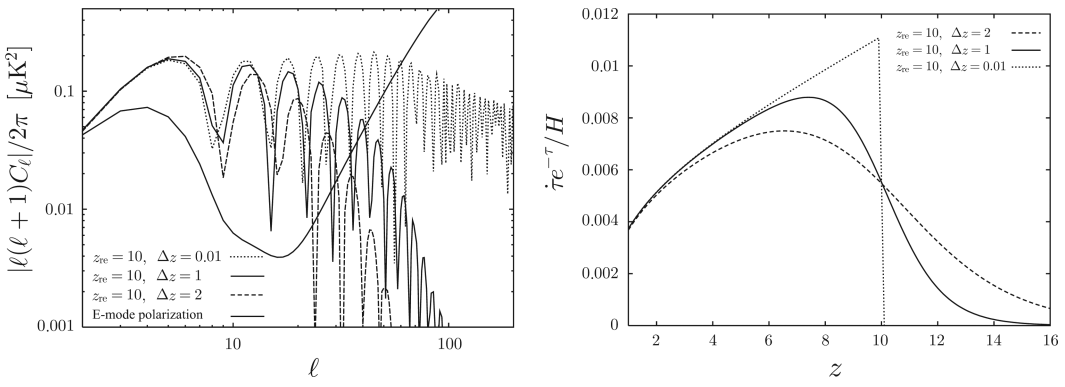

Figure 1. The left-hand panel shows the angular power spectra of the cross-correlation between E-mode polarization and 21-cm line fluctuations. We set $z_{\rm re} = 10, z_{\rm obs} = 10$ and $f = 0$ for all curves. The dotted line represents the angular spectrum for $\Delta z = 0.01$. The solid and dashed lines are for $\Delta z = 1$ and 2, respectively. For comparison, the thin solid line shows the angular power spectrum of the CMB E mode for $z_{\rm re} = 10$ and $\Delta z = 1$. The right-hand panel is the evolution of the visibility function $\dot{\tau}e^{-\tau}$ in the same reionization model as the left-hand panel. The dotted, solid and dashed lines are for $\Delta z = 0.01$, 1 and 2, respectively.

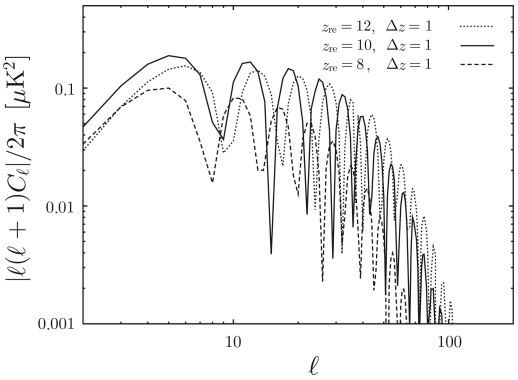

Figure 2. The angular power spectra of the cross-correlation between *E*-mode polarization and 21-cm line fluctuations. The dotted line is for $z = 12$. The solid and dashed lines are for $z = 10$ and 8, respectively. We use $\Delta z = 1, z_{\rm obs} = 10$ and $f = 0$ for all curves.

spherical Bessel functions have a steep cut-off after $\eta_{\rm obs}$ so that the contributions from epochs earlier than $\eta_{\rm obs}$ are negligible. Therefore, additional effective contributions come from only the former epoch $\eta < \eta_{\rm obs}$, and make the peak shift towards higher ℓ modes.

The major effect of Δz exhibited in the plot (left-hand panel of Fig. 1) is the damping at high ℓs with increasing durations of reionization. This occurs again due to the increase in the amplitude of the visibility function at $z > z_{\rm re}$. At high ℓs, the source term $P^{(0)}$ exhibits rapid oscillations. Since the tail of the visibility function is larger, the range of the integral is larger and it thus encompasses more oscillations. As a result, many more cancellations occur which damp the overall power. We note that the damping depends on the duration of the reionization which is an advantage of observing the cross-correlation signal. As a matter of fact, it is difficult to see differences among CMB polarization spectra for different durations, because the Thomson optical depth is not strongly sensitive to this parameter. However, the plots in the left-hand panel of Fig. 1, clearly show that the damping of angular spectrum of the cross-correlation is sensitive to the duration of reionization making it a potential tool for constraining this parameter of the reionization history.

We now vary the reionization redshift $z_{\rm re}$ keeping the other parameters fixed, and setting $z_{\rm obs} = 10, \Delta z = 1$ and $f = 0$. We find that increasing $z_{\rm re}$ shifts the position of the first peak to small scales (Fig. 2). The reason is the same as one invoked for the shifts observed in the left-hand panel of Fig. 1. When reionization happens early, the integration of the *E*-mode polarization in equation (14) takes into account more contribution from higher redshifts. This induces a shift of the peak position to higher ℓ modes.

Fig. 3 shows the evolution of the first peak amplitude as a function of $z_{\rm obs}$, the redshift of the 21-cm line emission, for the three above-mentioned durations of reionization Δz. Here, we set $z_{\rm re} = 10$ and $f = 0$. As shown by Alvarez et al. (2006) using equation (18), the amplitude of the cross-correlation of the CMB Doppler temperature anisotropies and the 21-cm line fluctuations reaches its maximum value at $z_{\rm re} = 10$, where the ionized fraction is about half. The same is true in the case of the cross-correlation of the 21-cm line fluctuations and *E*-mode polarization. The reason for this is that the CMB polarization is produced in the ionized regions whereas the 21-cm line fluctuations are associated with neutral regions. We note that the signal in Fig. 3 is smaller at lower redshifts than at higher redshifts. This is due to the fact that the 21-cm signal vanishes once reionization is completed, i.e. at redshifts smaller than $z_{\rm re}$. For higher redshifts ($z_{\rm obs} > z_{\rm re}$), the low-scattered quadrupole component of the *E* modes is suppressed like in the lower redshifts part, but the integration in the *E* modes picks up contributions from the reionization epoch and the *E* modes are correlated with a larger contribution of the 21-cm signal. As a result, the amplitude of the cross-correlation does not decline as steeply as for $z_{\rm obs} < z_{\rm re}$. The difference between the curves is easily interpreted. In the $\Delta z = 2$ case, full reionization takes longer to complete than in the $\Delta z = 1$ case. Therefore, neutral regions persist longer, broadening the

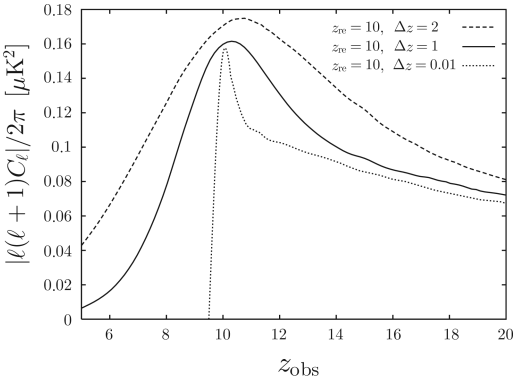

Figure 3. The amplitude of the first peak of the cross-correlation signal as a function of redshift $z_{\rm obs}$. The dotted, solid and dashed lines indicate the amplitudes for $\Delta z = 0.01$, 1 and 2, respectively. For all plots, we set $z_{\rm re} = 10$ and $f = 0$.

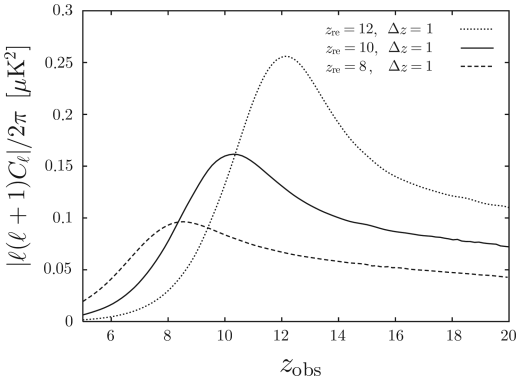

Figure 4. The evolution of the first peak amplitude for different $z_{\rm re}$. The dotted, solid and dashed lines represent the evolution for $z_{\rm re} = 12$, 10 and 8, respectively. In this figure, we assume $\Delta z = 1$ and $f = 1$.

skewed bell-shape of the curve centred on $z_{\rm obs} = z_{\rm re}$. The slight difference in the peak value is due to the cumulative effect of the integral in equation (14). This is particularly well illustrated by the case of 'instantaneous reionization' ($\Delta z = 0.01$). It is worth noting that our assumption, $T_{\rm s} \gg T_{\rm cmb}$, is formally not valid before the beginning of reionization. In order to evaluate the cross-correlation signal correctly, we should rather take into account the full evolution of $T_{\rm s}$ with redshift in the calculation of the 21-cm line fluctuations. However, by the time the ionization fraction has risen above the per cent level, efficient Compton and X-ray heating will guarantee that the spin temperature be well above $T_{\rm cmb}$ (e.g. Pritchard & Furlanetto 2007).

The evolution of the first peak amplitude for different $z_{\rm re}$ is shown in Fig. 4. As expected, the amplitude reaches its maximum value at each $z_{\rm re}$. Since the 21-cm optical depth is higher at high $z_{\rm obs}$, the amplitude of the 21-cm line fluctuations at higher redshifts is higher than that at lower redshifts. Therefore, and as exhibited by the comparison of the amplitudes for the different $z_{\rm re}$, the maximum value of the first peak cross-correlation amplitude is larger in the early reionization case than in the late reionization case. This again is the same evolution that shows up in the power spectrum of the cross-correlation between the CMB temperature anisotropy and the 21-cm line fluctuations (cf. fig. 2 of Alvarez et al. 2006). The evolution, with the observed redshift, of the shape and the amplitude of the first peak of cross-correlation between the 21-cm line fluctuations and *E*-mode fluctuations should allow us to constrain both the duration and redshift of reionization.

Ultimately, the parameter f is not independent of the epoch $z_{\rm re}$ of reionization and its duration Δz. However, making that dependency explicit would require the very detailed description of the reionization processes which we are still lacking today. We can nevertheless illustrate how the cross-correlation power spectrum changes for different global reionization scenarios. The left-hand panel in Fig. 5 shows the variation of the evolution of the first peak amplitude with the parameter f. There is no difference of the peak position in both spectra for the 'photon counting limit' $f = 0$ and the 'Strömgren limit' $f = 1$ but the amplitudes are different. When f increases, recombinations become more and more important. Accordingly, overdense regions in the case of $f = 0$ have higher ionization fraction than in the case of $f = 1$ as mentioned in Section 2.3. Since the fluctuations of the neutral fraction are defined by $\delta_{\rm H} = -\delta_x$, the absolute value of the 21-cm line fluctuations for $f = 0$ is higher than for $f = 1$. Therefore, the absolute value of the amplitude of the CMB *E*-mode anisotropies and the 21-cm line fluctuations correlation for $f = 0$ is higher than for $f = 1$ as shown in the left-hand panel of Fig. 5.

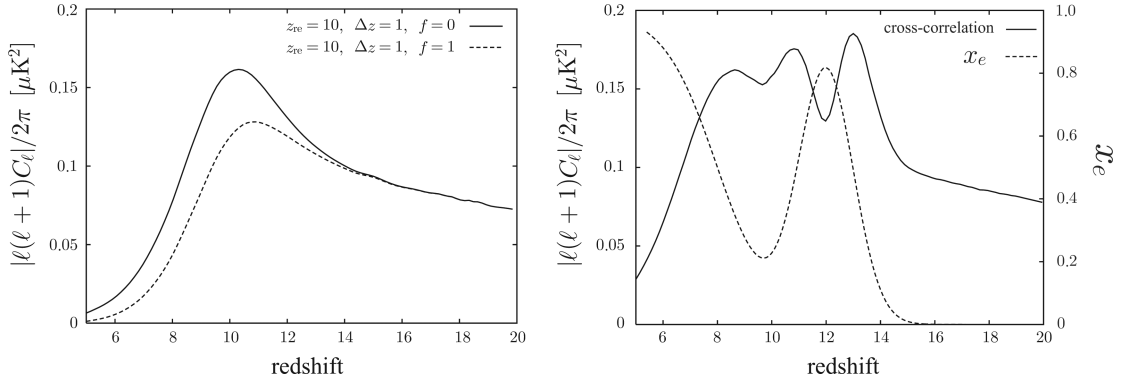

Figure 5. The left-hand panel shows the evolution of the first peak amplitude for two extreme values of the parameter f. The solid and dashed lines are for $f = 0$ and 1, respectively. We set $z_{\rm re} = 10$ and $\Delta z = 1$ in all plots. The right-hand panel shows the evolution of the first peak amplitude in the case of a double reionization model. The solid line (left axis) is for the first peak amplitude at given redshift. The dotted line (right axis) indicates the ionization fraction in the double reionization model.

Finally, we also calculate the cross-correlation between the 21-cm line fluctuations and the *E*-mode CMB anisotropies in the case of a double reionization. For illustrative purposes, we chose a simple parametrization of the mean ionized fraction

$$\bar{x}_{\rm e}(z) = 1 - \frac{1}{1+\exp[-(z-z_{\rm re})/\Delta z]} + A\exp\left[-\frac{(z-z_{\rm first})^2}{\Delta z^2_{\rm first}}\right], \quad (19)$$

which is the simple reionization case formula with $z_{\rm re} = 8$ and $\Delta z = 1$ on top of which we added a Gaussian with $A = 0.8$, $z_{\rm first} = 12$, and $\Delta z^2_{\rm first} = 2$ that encodes a first passage through an 80 per cent reionized universe at a redshift of 12. These parameters have been adjusted so as to reproduce the same value of the optical depth ($\tau = 0.08$) as the single reionization model shown in the left-hand panel of Fig. 5. The redshift evolution of $\bar{x}$ in this toy model is represented by the dashed line in the right-hand panel of Fig. 5 (read right axis for values of $\bar{x}_{\rm e}$). In the same figure, the solid line shows the corresponding evolution of the first peak of the cross-correlation (left axis). Every time the ionized fraction takes the value 0.5, there is a peak in the cross-correlation signal. In the case of our model for double reionization, we observe three peaks, i.e. the ionization fraction crosses the 0.5 line thrice. However, the two peaks at $z_{\rm obs} \sim 8$ and 11 are very close to each other. If two consecutive crossings of the 0.5 line occur very soon after each other, the corresponding peaks in the cross-correlation signal will be essentially indistinguishable. Similarly to what has been found by Alvarez et al. (2006), this behaviour is a very interesting property as it implies that we can use the 'trajectory' of the evolution of the peak amplitude to constrain the reionization model.

4 CONCLUSION

We have examined the cross-correlation between the *E*-mode CMB polarization and the fluctuations of the 21-cm line background. In particular, we calculated the angular power spectrum of the cross-correlation on large scales using a simple parametrization of reionization, focusing explicitly on the redshift $z_{\rm re}$ of its occurrence and on its duration Δz. We also considered the case of double reionization for which we obtained specific signatures.

The angular power spectrum of the cross-correlation traces the quadrupole component of the CMB temperature anisotropies at the redshift, where the 21-cm line is observed. Both the amplitude and the position of the first peak depend on the reionization epoch, as well as on the redshift $z_{\rm obs}$ probed by the 21-cm observations. We showed that the signal peaks when $z_{\rm obs}$ matches $z_{\rm re}$, in the very same way as does the cross-correlation between the CMB Doppler temperature anisotropies and the fluctuations of the 21-cm line background (see Alvarez et al. 2006), that is, when the 21-cm observations probe the epoch at which the ionized fraction becomes one-half. When probing higher redshifts, the polarization and 21-cm cross-correlation signal decreases slowly, whereas it falls off rapidly when lower redshifts $z_{\rm obs}$ are considered.

The location of the first peak in the ($z_{\rm obs}$–C_ℓ^{E-21}) plane is essentially independent of Δz. Therefore, tracking the evolution of the first peak amplitude by scanning the sky in $z_{\rm obs}$ bins would allow to determine $z_{\rm re}$. Moreover, the width of the bell-shaped curve describing the evolution with $z_{\rm obs}$ of the C_ℓ^{E-21} first peak depends on Δz. The duration of the reionization is thus also accessible through this observable quantity.

We also showed that, in addition to the amplitude and the position of the first peak, the duration of reionization induces a significant damping of the oscillations on small scales. This strong dependence on the duration shows specifically in the cross-correlation power spectrum as it does not arise in the auto-correlations power spectra.

These significant features, which are the oscillations and the maximum at the redshift when the ionized fraction are one-half, are explained by equation (14) which is an exact analytic expression. They are robust and independent of the details of the model. The assumptions are only introduced to relate the gravitational potential to the baryon density contrast and to the ionized fraction in equation (14). For the ϕ– $\delta_{\rm b}$ relation, we assume linear perturbation theory which is valid on large scales ($\ell > 100$) and at high redshift ($z \sim 10$). For the ϕ– δ_x relation, we need to assume a reionization model. We choose a simple model based on the halo model. In our redshift range when the reionized fraction is around one-half, as shown in many numerical studies (e.g. Iliev et al. 2006), the typical size of ionized bubbles is smaller than the instrumental resolution. In this case, we can assume that the ionized fraction can be set by the number of ionizing sources (for a detailed discussion see the appendix in Alvarez et al. 2006). The numerical simulations that provide detailed descriptions of the reionization history can test those assumptions.

In this study, we assumed the observation of the 21-cm line ideal. In practice, it amounts to consider that the frequency window function is the delta function $\delta(\nu - \nu_{\rm obs})$, implying that the observations are done at the specified frequency $\nu_{\rm obs}$ only. Of course, for real observations, the finite instrumental frequency width has to be taken into account. For too broad window functions, this is susceptible to induce an additional damping of the higher ℓ oscillations. We thus checked this effect in the case of the LOFAR interferometer that has a frequency width of 4 MHz. As a result, we did not obtain any additional significant damping of the oscillations for $\ell < 200$.

Both CMB and 21-cm signals suffer from the foreground contaminations. Some of them will be correlated like the synchrotron emission from our Galaxy. Recent studies have shown that the cleaning of foreground was under control in both CMB and 21 cm observations (Bock et al. 2006; Jelic et al. 2008). In addition, the multifrequency information on the CMB will allow the cross-correlation signal to be even less sensitive to the correlated foregrounds.

Finally, due to the cosmic variance that limits CMB measurements on large scales, it may actually be difficult to pinpoint the first peak with great accuracy. Moreover, ground-based telescopes designed for observations of the 21-cm line background cannot cover the whole sky. Those two facts are not important limitations for our study, since the damping of oscillations in the cross-correlation power spectrum on intermediate scales ($10 < \ell < 100$), which are well enough sampled, depends strongly on the reionization evolution. Actually, even if the reionization duration is so long that we cannot detect the oscillations due to the strong damping, it is still possible to obtain a lower limit for the duration. We will study this in more detail with numerical simulations in the future.

REFERENCES

Adshead P., Furlanetto S., 2008, MNRAS, 384, 291
Alvarez M. A., Komatsu E., Doré O., Shapiro P. R., 2006, ApJ, 647, 840
Barkana R., Loeb A., 2001, Phys. Rep., 349, 125
Benson A. J., Nusser A., Sugiyama N., Lacey C. G., 2001, MNRAS, 320, 153
Bharadwaj S., Ali S. S., 2004, MNRAS, 352, 142
Bock J. et al., 2006, preprint (astro-ph/0604101)
Cen R., 2003, ApJ, 591, 12
Ciardi B., Madau P., 2003, ApJ, 596, 1
Cooray A., 2004, Phys. Rev. D, 70, 063509
Cooray A., 2006, Phys. Rev. Lett., 97, 261301
Fan X. et al., 2006, AJ, 132, 117
Field G., 1958, Proc. IREE Aust., 46, 240
Furlanetto S. R., Oh S. P., Pierpaoli E., 2006, Phys. Rev. D, 74, 103502
Gunn J. E., Peterson B. A., 1965, ApJ, 142, 1633
Hu W., Sugiyama N., 1995, ApJ, 444, 489
Hu W., White M., 1997, Phys. Rev. D, 56, 596
Iliev I. T., Mellema G., Pen U.-L., Merz H., Shapiro P. R., Alvarez M. A., 2006, MNRAS, 369, 1625
Jelic V. et al., 2008, preprint (arXiv:0804.1130)
Kaiser N., 1987, MNRAS, 227, 1
Kodama H., Sasaki M., 1984, Prog. Theor. Phys. Suppl., 78, 1
Loeb A., Zaldarriaga M., 2004, Phys. Rev. Lett., 92, 211301
Madau P., Meiksin A., Rees M. J., 1997, ApJ, 475, 429
Page L. et al., 2007, ApJS, 170, 335
Press W. H., Schechter P., 1974, ApJ, 187, 425
Pritchard J. R., Furlanetto S. R., 2007, MNRAS, 376, 1680
Salvaterra R., Ciardi B., Ferrara A., Baccigalupi C., 2005, MNRAS, 360, 1063
Slosar A., Cooray A., Silk J. I., 2007, MNRAS, 377, 168
Spergel D. N. et al., 2007, ApJS, 170, 377
Tashiro H., Sugiyama N., 2006, MNRAS, 372, 1060
Tozzi P., Madau P., Meiksin A., Rees M. J., 2000, ApJ, 528, 597
Wouthusen S., 1952, AJ, 57, 31
Zaldarriaga M., 1997, Phys. Rev. D, 55, 1822

APPENDIX A: THE CMB *E*-MODE POLARIZATION

The source term of *E*-mode polarization in equation (2) (Hu & White 1997),

$$P^{(0)}(\eta, k) = \Theta_2^{(0)}(\eta, k) - \sqrt{6}E_2^{(0)}(\eta, k), \tag{A1}$$

where $\Theta_2^{(0)}$ is the quadrupole moment of the CMB temperature anisotropies.

The CMB temperature anisotropies are evaluated by the following integral solutions obtained from the Boltzmann equations,

$$\frac{\Theta_\ell^{(0)}(\eta_0, k)}{2\ell+1} = \int_0^{\eta_0} \mathrm{d}\eta e^{-\tau} \sum_{\ell'} S_{\ell'}^{(0)}(\eta) j_\ell^{(\ell')}[k(\eta_0 - \eta)], \tag{A2}$$

where the $j_\ell^{(\ell)}$ are expressed in terms of the spherical Bessel functions $j_\ell(x)$,

$$j_\ell^{(0)}(x) = j_\ell(x), \qquad j_\ell^{(1)}(x) = j_\ell'(x), \qquad j_\ell^{(2)}(x) = \frac{1}{2}[3j_\ell''(x) + j_\ell(x)], \tag{A3}$$

and $S_\ell^{(0)}$ are source terms written as

$$S_0^{(0)} = \dot{\tau}\Theta_0^{(0)} - \dot{\Phi}, \qquad S_1^{(0)} = \dot{\tau} v_\mathrm{B} + k\Psi, \qquad S_2^{(0)} = \frac{\dot{\tau}}{10}\left[\Theta_2^{(0)} - \sqrt{6}E_2^{(0)}\right], \tag{A4}$$

where v_b is the velocity of the baryon fluid, Φ and Ψ are the scalar-type metric perturbations in the conformal Newtonian gauge. The cosmological linear perturbation theory provides the evolution of Φ and Ψ and the initial condition of Θ_0 in the matter-dominated epoch as (Kodama & Sasaki 1984)

$$\Psi = -\Phi = -\frac{9}{10}\Psi(0), \qquad \Theta_0(0) = \frac{3}{5}\Psi(0), \tag{A5}$$

where Ψ (0) is the initial metric perturbation.

Before recombination, photons and baryons are tightly coupled by Compton scattering. Hence, the tight-coupling approximation is a strong tool for solving equations (2) and (A2). Hu & Sugiyama (1995) provided a useful analytic expression of the monopole component in this approximation,

$$\Theta_0(\eta) + \Phi(\eta) = [\Theta_0(0) + \Phi(0)]\cos kr_\mathrm{s}(\eta) - \frac{k}{\sqrt{3}}\int_0^\eta \mathrm{d}\eta'[\Phi(\eta') - \Psi(\eta')]\sin[kr_\mathrm{s}(\eta) - kr_\mathrm{s}(\eta')], \tag{A6}$$

where r_s is the integration of the sound speed $c_s = 1/\sqrt{3(1+R)}$,

$$r_s = \int \mathrm{d}\eta \frac{1}{\sqrt{3(1+R)}}. \tag{A7}$$

The dipole and quadrupole components, and the baryon velocity are written as

$$\Theta_1 = -\frac{3}{k}(\dot{\Theta}_0 + \dot{\Phi}), \qquad \Theta_2 = \frac{4\sqrt{4}}{9}\frac{k}{\dot{\tau}}\Theta_1, \qquad v_B = \Theta_1. \tag{A8}$$

Accordingly, the quadrupole component of E modes is given by

$$E_2 = -\frac{\sqrt{6}}{4}\Theta_2. \tag{A9}$$

After recombination, the tight-coupling approximation is no longer valid. Using equations (A5)–(A9) as initial conditions, we solve equations (2) and (A2) numerically in order to obtain the transfer function $D_E(k, \eta)$ in equation (3).

This paper has been typeset from a TEX/LATEX file prepared by the author.